

1
N1195-780

GODDARD
GRAIN

IN-37-TM

114226

P. 5

ORIGINAL PAGE IS
OF POOR QUALITY

TRAJECTORY CONTROL OF ROBOT MANIPULATORS
WITH CLOSED-KINEMATIC CHAIN MECHANISM

Charles C. Nguyen and Farhad J. Pooran
Center for Artificial Intelligence and Robotics (CAIR)
The Catholic University of America
Washington D.C.
and
Timothy Premack
NASA/Goddard Space Flight Center (GSFC)
Greenbelt, Maryland

ABSTRACT: This paper considers the problem of cartesian trajectory control of a closed-kinematic chain mechanism robot manipulator, recently built at CAIR to study the assembly of NASA hardware for the future space station. The study is performed by both computer simulation and experimentation for tracking of three different paths: a straight line, a sinusoid and a circle. Linearization and pole placement methods are employed to design controller gains. Results show that the controllers are robust and there are good agreements between simulation and experimentation. They also show excellent tracking quality and small overshoots.

1. INTRODUCTION

The control problem of robot manipulators can be considered to consist of two coherent subproblems: trajectory planning and trajectory control. Based on the coordinate system used in planning and controlling the robot hand trajectory, control schemes can be conveniently divided into two classes: joint space and cartesian space control schemes. In joint space control methods, the error actuating signal to the joint actuators is computed based on the error between the desired joint position and the actual joint position of the manipulator hand. On the other hand, the cartesian space-oriented methods use the error between the desired and actual cartesian position of the manipulator to compute the error actuating signal to the joint actuators [3]. While enjoying the simplicity in trajectory planning, the joint space-oriented method suffers from the difficulty in determining link locations of the robot hand during motion, a task requiring to ensure obstacle avoidance along the trajectory [3]. Furthermore, joint coordinates are not suitable as a working coordinate system because the joint axes of most manipulators are not orthogonal and they do not separate position from orientation [10]. The cartesian space-oriented approach whose path planning requires intensive computations for transformations between cartesian and joint coordinates in real time, has the advantage of assuring a certain degree of accuracy along the desired path and being more adaptable to the user.

There has been numerous interest in developing cartesian space-oriented control schemes. Considering that paths are made up by straight line segments, connected by smooth transition, Paul [10] and Taylor [15] proposed schemes that control the acceleration at the transition in order to achieve the desired cartesian path. Cartesian control of joint compliance manipulators was studied in [4]. The research in [6] and [17] shows that cartesian acceleration and force can be controlled successfully. Recently a closed-kinematic chain mechanism robot was built at NASA (Goddard Space Flight Center) to study the robotic assembly of NASA hardware for the future space station. This paper presents part of the ongoing robotic research at CAIR

for the control of the NASA robot. In particular, we consider the cartesian trajectory control of a small scale, manipulator with 2 degrees of freedom, resembling part of the complete NASA robot. Controllers are designed through the linearization of the robot dynamics and pole placement methods. The tracking performance of the controller will then be studied by both simulation and experimentation for three different trajectories: a straight line, a sinusoid and a circle. This paper is structured as follows. First we present the hardware of the manipulator under study together with the development of its kinematic and dynamic equations. Then the linearization about an operating point is discussed in conjunction with the controller design through the pole placement method. Finally we report the results of computer simulation and experimental study and make comparative evaluations.

2. THE MANIPULATOR MODEL

The main parts of the robot manipulator under study are presented in Fig. 1. It is a closed-kinematic chain mechanism manipulator with two degrees of freedom. Two links of the manipulator are composed of two ball-screw actuators, driven by two dc motors and hung below a fixed platform by means of pin joints. Two linear voltage differential transformers (LVDT) are mounted along the links to measure their lengths. The other ends of the links are joined together by a pin joint on which a gripper is mounted. The gripper motion is expressed with respect to a reference x-y cartesian coordinate system attached to the fixed platform as seen. The cartesian variables x and y are related to the joint variables l_1 and l_2 , the link lengths by [9]:

$$x = (l_1^2 - l_2^2 + d^2) / (2d) \quad (1)$$

$$\text{and } y = -[4d^2 l_1^2 - (l_1^2 - l_2^2 + d^2)^2]^{1/2} \quad (2)$$

where d is the distance between the pin joints hanging the actuators.

The Lagrangian equation of motion of a robot manipulator is given by:

$$F = M(l) \ddot{l} + H(l, \dot{l}) + G(l) \quad (3)$$

where F is a vector of input forces acting on the manipulator and l is a vector of joint variables. M(l), N(l, \dot{l}) and G(l) represent the moment of inertia, the centrifugal and coriolis forces, and the gravity, respectively. Using Lagrangian approach, we derive the following equations of motions:

$$F_1 = m_1 \ddot{l}_1 + [m_1 l_m (l_2 - l_1) / (3q)] \dot{l}_2 + G_1 \quad (4)$$

ORIGINAL PAGE IS
OF POOR QUALITY

$$F_2 = m_1 \ddot{l}_2 + [m_1 l_m (l_1 - l_2) / (3q)] \dot{l}_1 + G_2 \quad (5)$$

$$G_1 = -m_1 g [2B_1 l_1^2 (l_1 l_m + l_2 l_m + 2l_1 l_2) - l_2 l_m q^2] - m g l_m [2l_1^2 B_1 (l_1 + l_2) - l_2 q^2] / (4d l_1^2 l_2 q) \quad (6)$$

$$G_2 = -m_1 g [2B_2 l_2^2 (l_1 l_m + l_2 l_m + 2l_1 l_2) - l_1 l_m q^2] - m g l_m [2l_2^2 B_2 (l_1 + l_2) - l_1 q^2] / (4d l_1 l_2^2 q) \quad (7)$$

$$q = [4d^2 l_1^2 - (l_1^2 - l_2^2 + d^2)]^{1/2} \quad (8)$$

$$B_1 = l_2^2 - l_1^2 + d^2 \quad (9)$$

$$B_2 = l_1^2 - l_2^2 + d^2 \quad (10)$$

where m_1 is the mass of the moving part of the link, m is the total mass of the link, and l_m represents the fixed length of the actuators. Both actuators are assumed to be identical. In the derivation of the equations of motions the gripper is not included.

The Jacobian relating joint variable velocities \dot{l}_1 and \dot{l}_2 to cartesian velocity variables \dot{x} and \dot{y} is given by

$$J = \begin{bmatrix} l_1/d & -l_2/d \\ [(l_1 d^2 + l_1 l_2^2 - l_1^3) / (qd)] & [(l_2 d^2 + l_2 l_1^2 - l_2^3) / (qd)] \end{bmatrix} \quad (11)$$

The trajectory control scheme employed in this paper is presented in Fig. 2 where cartesian position feedback is obtained through the forward kinematic transform [Eqs. (1) and (2)]. Actual velocity is obtained by differentiating the actual position, which is implemented by the data acquisition software. The errors of cartesian position and velocity are converted into corresponding joint variable errors by means of the inverse Jacobian matrix. The joint variable errors will then serve as inputs to the PD controllers that in turn produce required forces for the actuators to track the robot gripper along a desired trajectory with a desired velocity profile.

3. LINEARIZATION AND CONTROLLER DESIGN

Since the dynamics of the manipulator is highly nonlinear, linearization about a selected operating point should be employed in order to design effective PD controllers. According to the work in [12], the linearization consists of expanding Eqs. (4) and (5) about a selected operating point using Taylor series expansion, neglecting higher order terms and transforming the resulting expression into a linear state equation given by:

$$\dot{z} = Az + BF \quad (12)$$

$$W = Cz \quad (13)$$

$$\text{where } z = (l_1 \ l_2 \ \dot{l}_1 \ \dot{l}_2)^T \quad (14)$$

$$\text{and } W = (l_1 \ l_2)^T \quad (15)$$

The development of A, B, and C can be found in [12]. From Fig. 2 we can write

$$F = P(v_1 - W) + D(v_2 - \dot{W}) \quad (16)$$

where P and D are matrices that contain parameters for the P controllers and D controllers, respectively and are given by

$$P = \begin{bmatrix} k_{p1} & 0 \\ 0 & k_{p2} \end{bmatrix} \quad D = \begin{bmatrix} k_{d1} & 0 \\ 0 & k_{d2} \end{bmatrix} \quad (17)$$

The vector v_1 and v_2 are command vectors expressing the desired joint variables and velocities, respectively. Substituting (16) into (12) and employing (13), after some manipulation we obtain

$$\dot{z} = (I + BDC)^{-1} (A - BPC)z + (I + BDC)^{-1} BQv \quad (18)$$

where

$$Q = \begin{bmatrix} P & 0 \\ 0 & D \end{bmatrix} \quad (19)$$

$$\text{and } v = (v_1 \ v_2)^T \quad (20)$$

From (18) it is obvious that the matrices P and D should be selected such that the eigenvalues of $(I + BDC)^{-1}(A - BPC)$ are stable, which can be realized by several available methods of pole placement and softwares. Particularly the procedures proposed in [13] is recommended. Here we assume that the matrix $(I + BDC)$ is nonsingular.

4. SIMULATION AND EXPERIMENTAL STUDY

In order to exam the performance of the cartesian control scheme illustrated in Fig. 2, we conducted both simulation and experimental study for tracking of three different trajectories: a straight line, a sinusoid and a circle. In the simulation study, the entire control scheme including the manipulator dynamics was simulated on an IBM/XT using the System Simulation Language (SYSL). First PD controller gains were selected using the procedures discussed in Sect. 2 to ensure the system stability. Then the obtained gains were adjusted for each of the above three tracking cases until a satisfactory tracking was achieved. According to the simulation results, the gain adjustments were within 10% of the original gains obtained from the linearization and pole placement methods. In the experimental study, the robot manipulator was interfaced with the IBM computer through a data acquisition system consisting of an IBM board, an adapter and a software called Labtech [7]. PD controllers, inverse Jacobian and the forward kinematic transform were implemented using Labtech. The gains obtained through the simulation study were applied to the real-time control of the robot manipulator. In the following we will present the above study results and make comparative evaluations:

Numerical Values:

(a) Linearization about the home position [$l_1 = 83.80$ cm, $l_2 = 85.90$ cm]:

$$A = \begin{bmatrix} 0 & 0 & 1 & 0 \\ 0 & 0 & 0 & 1 \\ -45.66 & 17.97 & 0 & 0 \\ 33.53 & -48.34 & 0 & 0 \end{bmatrix}$$

ORIGINAL PAGE IS
OF POOR QUALITY

$$B = \begin{bmatrix} 0 & 0 \\ 0 & 0 \\ 1.7 & 0 \\ 0 & 1.7 \end{bmatrix} \quad C = \begin{bmatrix} 1 & 0 & 0 & 0 \\ 0 & 1 & 0 & 0 \end{bmatrix}$$

(b) Controller Gains: $k_{p1} = 2400 \text{ N/m}$; $k_{p2} = 2600 \text{ N/m}$; $k_{d1} = 20 \text{ N.s/m}$;
 $k_{d2} = 20 \text{ N.s/m}$.

(c) Robot Dynamics: $m_1 = .59 \text{ kg}$; $m = 4.91 \text{ kg}$; $d = .737 \text{ m}$.

Tracking a straight line:

In this study the robot is to track a desired straight line described by the equation $y(t) = -x(t) - 42 \text{ cm}$ with a desired velocity of 1.7 cm/s . Figure 3 presents the simulation and experimental results for this case. The simulated motion follows the target path very closely with a maximum deviation of 4 mm . Experimental results show that the robot actually follows the desired path with an excellent tracking quality with some disturbances at the starting position. After reaching the steady state, the robot tracks the desired path very closely with a maximum deviation of 3 mm . The simulation and actual velocities in x and y directions are presented in Figures 4 and 5, respectively. As seen from these figures, both simulation and actual velocities lag behind the desired one. The simulation and actual velocities stay constantly at about 76% and 31% of the desired one, respectively.

Tracking a sinusoid:

The simulation and experimental results for tracking a sinusoidal trajectory described by the equation $y = 2.5 \sin(2x - 50) - 82.5 \text{ cm}$ with a desired constant velocity of 1.7 cm/s are shown in Figure 6. The simulation motion follows the desired trajectory very closely with a constant deviation of 3 mm . Actual motion shows good tracking quality with some disturbances during the transient state.

Tracking a circular path:

In this case we study the performance of the robot in tracking a circular trajectory described by the equation $(x - 13.5)^2 + (y + 33)^2 = 14$ with a desired constant velocity of 1.7 cm/s . Simulation motion agrees with the desired trajectory very closely with some insignificant shifting. Experimental results show that the actual motion of the robot resembles a circular path that is shifted to the left (horizontally) of the desired trajectory and is compressed vertically. The horizontal shifting and vertical compression are about 5 mm and 3 mm , respectively.

Evaluations and discussions:

The existence of the tracking errors in the above study cases can be clarified by the following reasons:

(a) The employed software and the computer are not capable of performing fast computations and high sampling rates. Because the data acquisition system has been using a sampling rate of 3 samples/sec, the feedback information provided by the position sensors (LVDT) cannot be updated quickly enough for the controller to act on the actuators. Thus the actual position of the robot cannot be updated timely, causing motion overshoots. The tracking quality can be improved tremendously if a data

acquisition system with faster computation capability and higher sampling rate is employed.

(b) As expected from most industrial and educational robots, our robot also suffers from some problems in machine design such as vibration, backlash, nonidentical actuators, and joint friction. These problems create tracking errors and can be remedied by improving the machine design or applying a more advanced control scheme such as adaptive control.

5. CONCLUSION

In this paper we have considered the problem of cartesian trajectory control of a closed-kinematic chain mechanism robot manipulator with two degrees of freedom. Linearization and pole placement methods were employed to design the PD controller gains. The performance of the control scheme was examined by both simulation and experimentation. Study results showed good agreements between simulation and experimentation. They also showed that appropriate adjustments of controller gains designed from a linearized model of a robot manipulator enables one to design effective controllers for this manipulator. Since the linearized model is only valid in the neighborhood of a selected operating point, the tracking can be improved if there exists a scheme to update the controller gains by updating the linearized model as the manipulator moves along the path. Current active research at CAIR is focused on the analysis and implementation of an adaptive control scheme for the above robot manipulator.

6. ACKNOWLEDGMENTS

The authors of this paper wish to express their thanks to NASA (Goddard Space Flight Center) for supporting the research of this paper under the research grant # NAG 5-780.

7. REFERENCES

1. Brady, Michael, "Trajectory Planning", in Robot Motion: Planning and Control, Brady, M. et al, Eds, MIT Press, Cambridge Massachusetts, 1983.
2. Craig, John J., Introduction to Robotics, Addison Wesley, 1986.
3. Fu, K. S. et al, Robotics: Control, Sensing, Vision, and Intelligence, McGraw-Hill, 1987.
4. Hill, S. P., and Vaccaro, R. J., "Cartesian Control of Robotic Manipulators with Joint Compliance," Proc. IEEE Int. Conference on Robotics and Automation, 1985, pp.114-120.
5. Khatib, O. "A Unified Approach for Motion and Force Control of Robot Manipulators: The Operational Space Formulation," IEEE Journal of Robotics and Automation, Vol. RA-3, February 1987, pp. 43-53.
6. Luh, J. Y. S. et al, "Resolved-Acceleration Control of Mechanical Manipulators," IEEE Trans. Automatic Control, vol.AC-25, no. 3, pp. 468-474.
7. Nguyen, C. C. and Pooran, F. J. "Development of Hardware and Computer Interface of a Two-degree-of-freedom Robot", NASA Report, Grant # NAG 5-780, June 1987.

8. Nguyen, C. C., Pooran, F. J. and Premack, T., "Modified Hybrid Control of Robot Manipulators for High Precision Assembly Operations," ISM International Conference Computer Applications in Design, Simulation and Analysis, Honolulu, Hawaii, Feb. 1987.

9. Nguyen, C. C., Pooran, F. J., and Premack, T., "Control of Robot Manipulator Compliance," in Recent Trends in Robotics: Modeling, Control and Education, Chapter 2, edited by M. Jamshidi, J. Y. S. Luh and M. Shahinpoor, North Holland, 1986.

10. Paul, Richard, P. C., "Manipulator Cartesian Path Control", IEEE Transaction on Systems, Man and Cybernetics, SMC-9 (1979), pp. 702-711.

11. Saridis, G. N., Advances in Automation and Robotics, Vol. I, JAI Press Inc., Connecticut, 1985.

12. Seraji, H., et al, "Linear Multivariable Control of Two-Links Robots," Journal of Robotic Systems, 3(4), 1986, pp. 349-365.

13. Seraji, H., "Pole Placement in Multivariable Systems Using Proportional-Derivative Output Feedback," Int. J. Control, Vol. 31, No. 1, 1980, pp. 195-207.

14. Shin, Kang G., "Robust Trajectory Planning for Robotic Manipulators Under Payload Uncertainties," IEEE tran. Automatic Control, Vol. AC-32, No. 12, 1987, pp. 1044-1054.

15. Taylor, Russel H., "Planning and Execution of Straight line Manipulator Trajectories," in Robot Motion, Planning and Control, Brady et al, eds, MIT Press, 1983.

16. Whitney, D. E., "Resolved Motion Rate Control of Manipulators and Human Prostheses," IEEE Trans. Automatic Control AC-14, 1969, pp. 572-574.

17. Wu, C. H., and Paul, R. P., "Resolved Motion Force Control of Robot Manipulators," IEEE Trans. Systems, Man, Cybern., vol. SMC-12, no. 3, pp. 266-275.

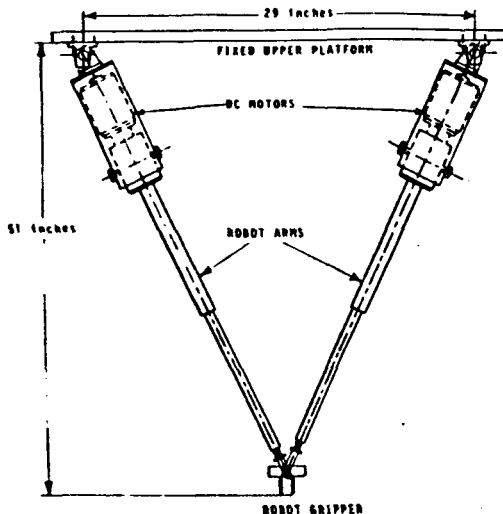


Fig. 1: The closed-kinematic chain mechanism robot manipulator

ORIGINAL PAGE IS
OF POOR QUALITY

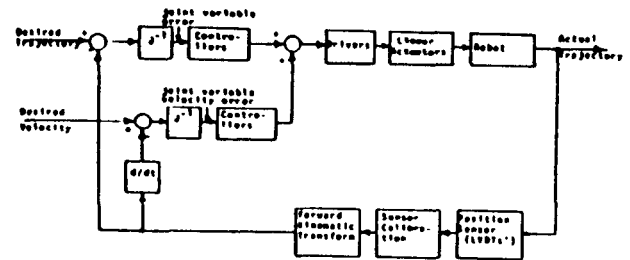


Fig. 2: Cartesian trajectory control of the robot manipulator

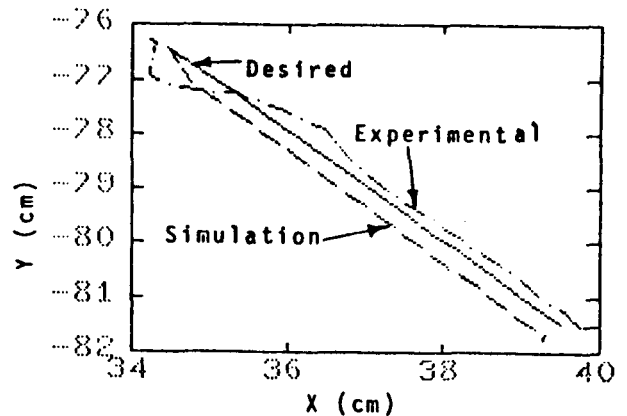


Fig. 3: Case study of the straight line trajectory

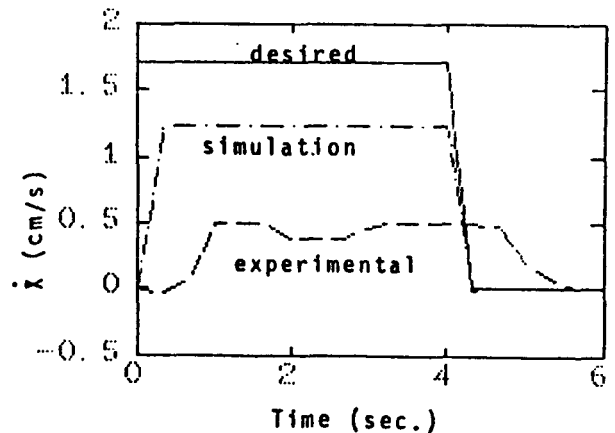


Fig. 4: Horizontal velocity for the straight line case

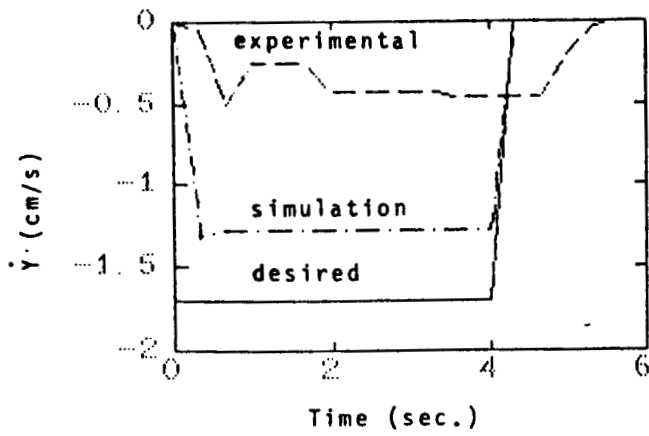


Fig. 5: Vertical velocity for the straight line case

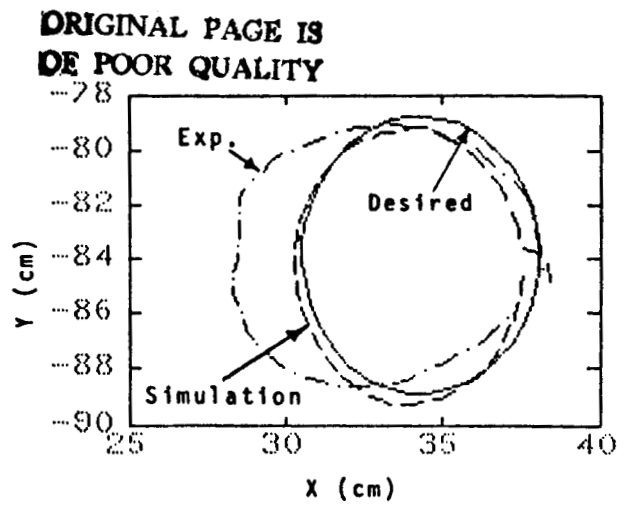


Fig. 7: Case study of the circular trajectory

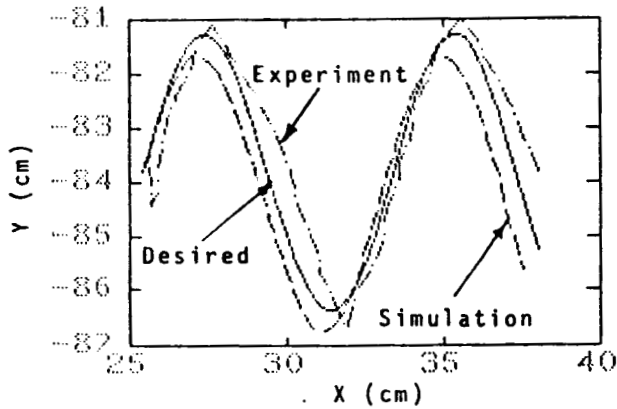


Fig. 6: Case Study of the sinusoidal trajectory